ELSEVIER

Journal of Nuclear Materials 254 (1998) 135–142

journal of nuclear materials

The influence of neutron irradiation on the microstructure of Al_2O_3, $MgAl_2O_4$, $Y_3Al_5O_{12}$ and CeO_2

R.J.M. Konings [a], K. Bakker [a,*], J.G. Boshoven [a], R. Conrad [b], H. Hein [a]

[a] *Netherlands Energy Research Foundation ECN, P.O. Box 1, 1755 ZG Petten, The Netherlands*
[b] *CEC Joint Research Centre IAM, P.O. Box 2, 1755 ZG Petten, The Netherlands*

Received 7 August 1997; accepted 20 November 1997

Abstract

Pellets of the ceramics Al_2O_3 (alumina), $MgAl_2O_4$ (spinel), $Y_3Al_5O_{12}$ (YAG) and CeO_2 (ceria) have been prepared and characterized. These pellets have been irradiated in the High Flux Reactor (HFR) in Petten during four reactor cycles (101.1 full power days), corresponding to a neutron fluence ($E > 0.1$ MeV) of 4.6×10^{25} m^{-2}. By post-irradiation examination the swelling of the pellets has been derived from the changes in geometry, and the influence of neutron irradiation on the microstructure has been studied using optical microscopy, scanning electron microscopy (SEM) and transmission electron microscopy (TEM). The results have been compared with literature data. © 1998 Elsevier Science B.V.

PACS: A05; N01; R02

1. Introduction

Partitioning and transmutation (P&T) of minor actinides are presently being studied as a complementary option in the management of high-level nuclear waste. It involves the separation of the actinides from spent fuel and subsequent re-irradiation in nuclear reactors to reduce the long-term radiotoxicity as well as the risk during storage. There is general agreement that the implementation of P&T in waste management is feasible but many technological issues have still to be solved. In Europe the cooperation within the EFTTRA (Experimental Feasibility of Targets for TRAnsmutation) collaboration [1] has been initiated to study the technological aspects of the transmutation of americium and the fission products Tc and I.

Two ways are generally considered for the transmutation of the actinides: homogeneous mixing in fresh fuel or heterogeneous mixing with a support material, which can be a ceramic or a metallic material. Homogeneous mixing can be considered as an adaption of mixed oxide fuel and can be implemented with some modifications of present technology. However, due to dose limitations it cannot be used for americium fuels. Heterogeneous mixing is also attracting much attention at present as the amount of plutonium and minor actinides formed during irradiation will be relatively low due to the absence of ^{238}U. However, a new technology for the fabrication of fuels is required before implementation of this option can be achieved.

The selection criteria for the support materials for actinide fuels are discussed by Cocuaud et al. [2] who concluded that the stability under irradiation (neutrons α-particles, recoil atoms or fission product stopping) is a major source of uncertainty. Among the possible candidates considered are Al_2O_3, $MgAl_2O_4$, $Y_3Al_5O_{12}$ and CeO_2. In the present investigation (EFTTRA-T2bis irradiation experiment) the behavior of these materials during in-pile neutron irradiation in the High Flux Reactor (HFR) in Petten is studied.

2. Experimental

2.1. Fabrication

A specification of the purities and the powder sizes of the four materials discussed is given in Table 1. The

* Corresponding author.

PII S0022-3115(97)00355-3

Table 1
The characteristics of the four types of pellets

Material	Vendor	Purity	Powder size
Al_2O_3	ALCO CT3000sg	$\simeq 99.80\%$[a]	0.6–0.8 μm
$MgAl_2O_4$	Baikowski C28CR	$\geq 99.9\%$	?[b]
$Y_3Al_5O_{12}$	Gimex	$\geq 99.9\%$	1 μm
CeO_2	Cerac	$\geq 99.9\%$[c]	< 50 μm

[a] Typical impurities Na_2O 0.08%, CaO 0.02%, SiO_2 0.03%, Fe_2O_3 0.02%, MgO 0.08%.
[b] The powder size after spray-drying has not been determined, but it is much smaller than that of the original powder (1–8 μm).
[c] All metallic impurities less than 20 ppm, except La 85 ppm.

aluminium oxide pellets were prepared from Al_2O_3 powder, which was pressed to a rod with a diameter of 13 mm by cold isostatic pressing. No lubricant was used for preparing the Al_2O_3 rod. The rod was presintered at 1000°C in air. After this preheating the rod was processed into pellets which were finally sintered at 1600°C in air. The $MgAl_2O_4$ pellets were prepared from $MgAl_2O_4$ powder, which was spray-dried to improve the sinterability. The $MgAl_2O_4$ suspension used for spray-drying was made by mixing 50 g of $MgAl_2O_4$ powder with 200 ml water and 1 ml of 3 M nitric acid. The spray-dried powder was pressed to pellets which were subsequently sintered at 1600°C for 10 h in air. The $Y_3Al_5O_{12}$ pellets were prepared from $Y_3Al_5O_{12}$ powder, which was pressed to rods with a diameter of 13 mm by cold isostatic pressing. No lubricant was used for preparing the $Y_3Al_5O_{12}$ rod. The rods were then presintered at 1000°C in air. After cooling down the rod was mechanically processed to the right diameter and cut into pellets, which were finally sintered at 1600°C in air. For the fabrication of the CeO_2 pellets, CeO_2 powder was mixed with a plasticizer (2 wt% Hoechst wax C micropulver PM) to improve the pressing performance. These pellets were sintered in air at 1600°C for 10 h, which resulted in slightly red pellets. During sintering the plasticizer was fully oxidized.

2.2. Characterization

All pellets were characterized before transfer into the irradiation capsules, using the following techniques: X-ray diffraction, measurements of the dimensions and weight, mercury porosimetry, optical microscopy, scanning electron microscopy (SEM) and transmission electron microscopy (TEM). The average grain sizes of the sintered pellets before irradiation were deduced from SEM images. These data are shown in Table 2, together with the initial densities of the pellets that have been determined from the weight and dimension measurements of the pellets.

All samples are single-phase according to X-ray analysis. The lattice parameter of a CeO_2 pellet has been determined by X-ray analysis in order to analyze the Ce/O-ratio. Chiang et al. [3] observed that the CeO_{2-x} $(0 \leq x \leq 0.2)$ lattice parameter increases strongly on a decreasing oxygen concentration. For the CeO_2 pellet used for the present study the room temperature lattice parameter is (0.54109 ± 0.00005) nm, which is in good agreement with the lattice parameter that Chiang et al. [3] observed for $CeO_{2.000}$ (0.54111 nm). Due to the poor pressing and sintering behavior of the CeO_2 pellets the mean technical density is only 83%. The SEM and optical microscopy photos show that the CeO_2 pellets have a bimodal porosity distribution, with pore sizes of 2–5 μm and of 100–150 μm. The large pores were formed by the evaporation of the plasticizer that was used to improve the pressing characteristics of the CeO_2 powder. Mercury porosimetry has been used to determine the open porosity in all four ceramic types. It was found that none of these ceramics contains open porosity, which is rather surprising in the case of CeO_2 which has a density of only 83%. However, the porosity in CeO_2 has a spherical shape, and the small pores are positioned intragranular, which prevents the formation of open porosity. TEM images show that none of the grains in these ceramics contained dislocation loops or bubbles prior to irradiation, except for $Y_3Al_5O_{12}$ in which some edge-type dislocations were observed.

2.3. Irradiation conditions

The Al_2O_3, $MgAl_2O_4$ and $Y_3Al_5O_{12}$ pellets were encapsulated in Zircaloy-4 tubes with an inner diameter of 9.30 mm and an outer diameter of 10.76 mm. The CeO_2 pellets were encapsulated in a stainless steel 316L tube with an inner diameter of 5.33 mm and an outer diameter of 6.3 mm. The height of the four pellet stacks was 50 mm. The capsules were filled with helium gas and were laser welded. X-ray radiographs and diameter measurements were made of the closed capsules prior to irradiation and no irregularities were observed.

The samples were irradiated in a central in-core position of the HFR-Petten during four reactor cycles (101.1 full power days). The neutron fluence was monitored by means of gamma-scan wires and fluence detector sets. The results of the post-test analysis of the neutron fluence monitoring showed that the neutron fluence ($E > 0.1$ MeV) was 4.6×10^{25} m^{-2} and the fast fluence ($E > 1.0$ MeV) was 2.2×10^{25} m^{-2}. The temperature in the sample holder

Table 2
The characteristics of the four types of pellets

Material	Grain size	Initial density	Diameter	Height
Al_2O_3	2 μm	96.4%	9.1 mm	10.0 mm
$MgAl_2O_4$	1 μm	95.6%	9.0 mm	4.8–5.0 mm
$Y_3Al_5O_{12}$	4 μm	94.0%	9.0 mm	10.2 mm
CeO_2	40 μm	83%	5.15 mm	5.2–5.9 mm

was measured by twelve thermocouples positioned close to the samples. During the four irradiation cycles the temperature was (710 ± 10) K.

2.4. Microscopy

The unirradiated and the irradiated pellets were cut, embedded in Hysol, grazed with SiC-paper and polished with diamond paste. Some of the samples have been etched cathodically. The pellets were examined by optical microscopy and SEM.

TEM samples were prepared by crushing small pieces of the unirradiated and the irradiated pellets using a mortar. The particles thus obtained were placed on a microscopy microgrid and covered with a thin plastic foil in order to prevent contamination of the microscope. The unirradiated powder was examined as a comparison to confirm that the observed microstructure in the irradiated powder was not induced by the powdering process or already present before the irradiation. The samples were studied in a Philips 301 TEM operated at 100 kV. Both bright field images and electron diffraction patterns were recorded.

3. Irradiation induced changes

In all four materials no differences were observed between the optical microscopy and SEM images as made before and after the irradiation. The electron diffraction patterns as obtained by TEM of both unirradiated and irradiated powders of the four ceramics showed no differences between the patterns of the unirradiated and the irradiated materials. This indicates that no extensive amorphization or cation/anion disorder is induced in the samples. The swelling measurements and the TEM bright field images of the four ceramics will be discussed in the next sections.

Comparing the data on the irradiation induced changes obtained from literature with the present results should be done carefully. Firstly, the impurity concentrations and the microstructures of the materials are not identical and secondly, the experimental conditions are not identical. Most of the literature data on the influence of neutron irradiation on Al_2O_3, $MgAl_2O_4$ and $Y_3Al_5O_{12}$ were obtained from experiments that were meant to test the applicability of these ceramics as fusion reactor components. These experiments were performed in fast reactors, such as FFTF, JOYO and EBR-II. The neutron spectra and the neutron fluxes in these reactors are different from those in the HFR, in which the present experiments were performed. The irradiation conditions of the experiments described in the literature are mentioned only very briefly in the articles. In most cases only the reactor in which the irradiation was performed and the neutron fluence ($E > 0.1$ MeV) are mentioned. Hence, it is impossible to make a detailed comparison of the irradiation conditions, and consequently of the irradiation induced changes.

Another parameter that complicates the comparison of the irradiation induced swelling or the changes in the microstructure is the variation in temperature at which the irradiation experiments have been performed. The swelling of ceramics depends on the irradiation temperature and has in general a maximum due to the combination of counteracting processes. An increase of the temperature induces an increase of the vacancy mobility, which enhances the swelling. However, an increase of the temperature also induces a decrease of the vacancy sink stability, which reduces the swelling above the temperature of the maximum [21]. The data obtained in the present study have been compared with literature data at approximately the same temperature.

3.1. Al_2O_3

For the five Al_2O_3 pellets an average swelling of 1.9% has been determined from the measurement of the dimensions. Good agreement is observed with literature data (Fig. 1, Table 3) on samples irradiated at approximately the same temperature as the present study, taking into account the variations in microstructure and irradiation conditions of the various experiments. The swelling data reported by Keilholtz et al. [7] deviate from the other data sets, which might be due to separation of the grains at the grain boundaries. Keilholtz et al. [7] mentioned only the fast component ($E > 1$ MeV) of the neutron fluence. The fluence $E > 0.1$ MeV is approximated in the present study as double the fast fluence value.

The influence of the irradiation temperature on the swelling of Al_2O_3 is rather unclear. Hobbs [21] suggested a very strong temperature dependence of the swelling, with

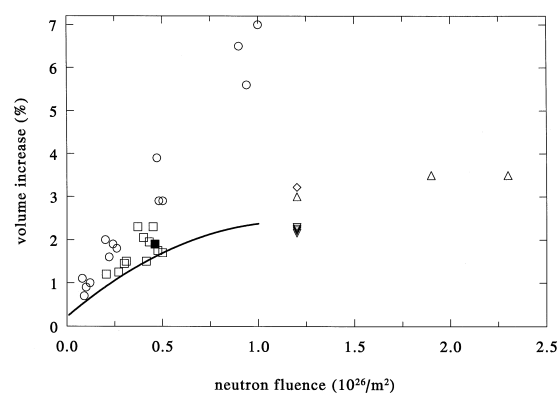

Fig. 1. The swelling of polycrystalline Al_2O_3 as a function of neutron fluence ($E > 0.1$ MeV): ◇, $T = 660$ K. Tucker et al. [4]; △, $T = 925$ K, Clinard et al. [5]; solid line, $T = 673$–823 K, Dienst [6]; ○, $T = 673$–853 K, Keilholtz et al. [7]; ▽, $T = 658$ K, Pells et al. [26]; □, $T = 650$–875 K, Clinard et al. [24]; ■, $T = 710$ K, present study.

Table 3
The swelling of Al_2O_3 as determined by various authors

Fluence ($E > 0.1$ MeV)[a] ($\times 10^{26}$ m^{-2})	Reactor	Temperature (K)	Material[a]	Initial density	Swelling	Authors
0.01–1	?	673–823	p.c.	?	0.2 to 2.4%	Dienst et al. [6]
0.1–1	ETR	673–853	p.c.	97–100%	0.7 to 7%	Keilholtz et al. [7]
0.25–0.5	EBR-II	650–875	p.c.	99%	1 to 3%	Clinard et al. [24]
0.3–2.3	EBR-II	430–1100	s.c.		1.7 to 4.4%	Clinard et al. [5]
0.46	HFR	710	p.c.	96.4%	1.9	present study
1.2	EBR-II	660	p.c.	$\pm$98%[b]	3.22%	Tucker et al. [4]
1.2	EBR-II	658	p.c.	97.5–99.7%	2.1 to 2.3%	Pells et al. [26]
1.2–2.3	EBR-II	925	p.c.	97%	3.0 to 3.5%	Clinard et al. [5]
2.2	EBR-II	680–815	s.c.		3.3 to 3.5%	Clinard et al. [14]
17	PHENIX	?	p.c.	?	28%	see Cocuaud

[a] p.c. marks polycrystalline and s.c. marks single-crystalline.
[b] This value is inaccurate since it could only be obtained from a graph.

a maximum around 950 K. Keilholtz et al. [7] observed an increase of the radiation damage in the temperature range from 373–873 K, while in the temperature range 873–1343 K, temperature was observed to have little effect on the damage. Clinard et al. [24] found that the swelling at 875 K was similar to that at 1025 K, while the swelling at 650 K was smaller than that at the two other temperatures. At higher neutron fluences Clinard et al. [5] observed that the swelling at 1100 K is approximately double the swelling at 925 K.

The TEM examination of the irradiated Al_2O_3 samples showed a high density of dislocation loops (Fig. 2). This observation is in agreement with literature data that exist on the behavior of Al_2O_3 under neutron irradiation [4,5,8,9] in a wide range of neutron fluences (0.3×10^{26}–2.1×10^{26} m^{-2}) and temperatures (400–1100 K). These studies showed that the swelling of irradiated Al_2O_3 is accompanied by dense dislocation networks and aligned voids [5].

3.2. $MgAl_2O_4$

For the ten $MgAl_2O_4$ pellets a volume change of -0.6% has been determined from the dimensional changes. Previous results on the influence of neutron irradiation on

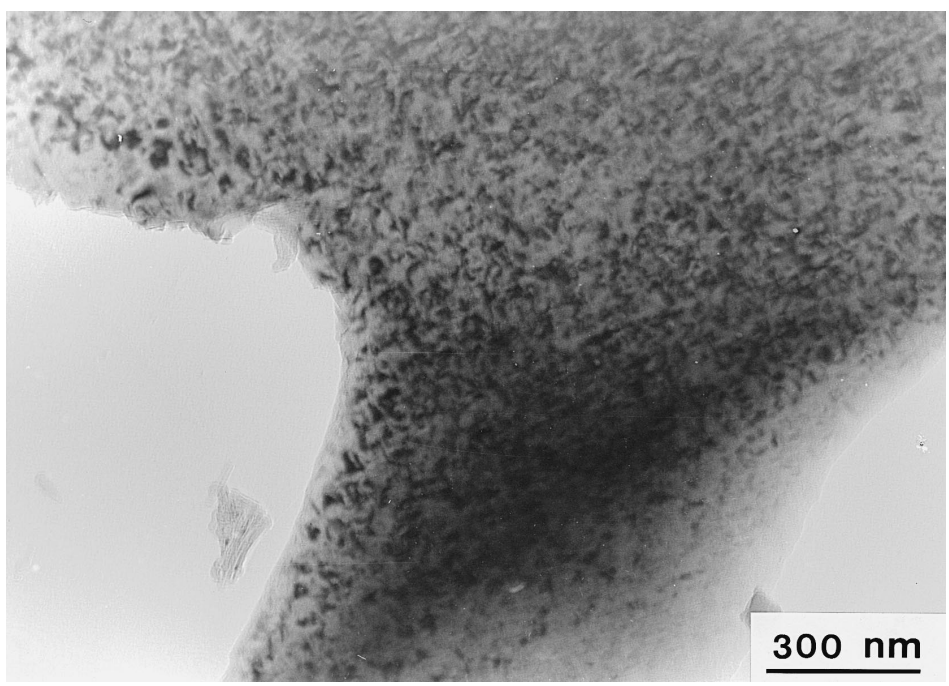

Fig. 2. TEM image of neutron irradiated Al_2O_3 (4.6×10^{25} m^{-2}).

Table 4
The swelling of $MgAl_2O_4$ as determined by various authors

Fluence ($E > 0.1$ MeV)[a] ($\times 10^{26}$ m^{-2})	Reactor	Temperature (K)	Material[a]	Initial density	Swelling	Authors
0.3, 2.3	EBR-II	925–1100	p.c.	> 99%	0.2 to 1.6%	Clinard et al. [5]
0.3–2.3	EBR-II	925–1100	s.c.		0 to 0.1%	Clinard et al. [5]
0.46	HFR	710	p.c.	95.6%	−0.60%	present study
1.2	EBRII	660	p.c.	95%[b]	−0.316%	Tucker et al. [4]
1.2	EBR-II	658	s.c.		−1.18%	Pells et al. [26]
2.1	EBR-II	430	p.c.	94%	0.8%	Clinard et al. [5]
2.2	EBR-II	680, 815	p.c.	99%	−0.35 to −0.19%	Clinard et al. [14]
2.2	EBR-II	680, 815	s.c.		−0.11 to −0 05%	Clinard et al. [14]
22.9	FFTF	658, 1023	s.c.		0 to 0.07%	Fukumoto et al. [15]

[a] p.c. marks polycrystalline and s.c. marks single-crystalline.
[b] This value is inaccurate since it could only be obtained from a graph.

the swelling of spinel are summarized in Table 4 and Fig. 3. In the single crystals almost no dimensional changes occur, except for the sample of Pells et al. [26], which showed a relatively large densification. Polycrystalline spinel irradiated at high temperatures (925–1100 K) showed some swelling. Of the samples irradiated in this temperature range the sample irradiated at the highest temperature showed the largest swelling (1.6% for 2.3×10^{26} m^{-2} at 1100 K). A spinel sample irradiated at low (430 K) temperature also showed some swelling [5]. The studies of Clinard et al. [14], Tucker et al. [4] and the present study were performed on polycrystalline samples irradiated in approximately the same temperature range (660–815 K). All these spinel samples showed a slight densification during irradiation. The somewhat larger densification of the spinel samples used in the present study might be due to their somewhat lower initial density.

The TEM images of the present study show no effect of irradiation to 4.6×10^{25} m^{-2} at 710 K on the microstructure of $MgAl_2O_4$. Various authors have performed TEM investigations on neutron irradiated $MgAl_2O_4$ [4,5,13–17,25], both on polycrystalline and single-crystalline material in a wide range of neutron fluences (1×10^{24}–2.3×10^{27} m^{-2}) and temperatures (430–1100 K).

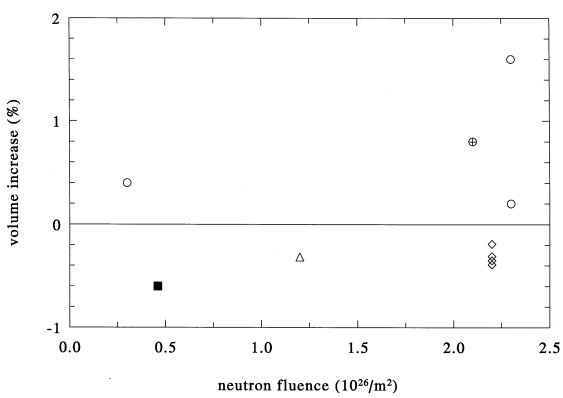

Fig. 3. The swelling of polycrystalline $MgAl_2O_4$ as a function of neutron fluence ($E > 0.1$ MeV): △, $T = 660$ K, Tucker er al. [4]; ⊕, $T = 430$ K, Clinard et al. [5]; ○, $T = 925$–1100 K, Clinard et al. [5]; ◇, $T = 680$, 815 K, Clinard et al. [14]; ■, $T = 710$ K, present study.

These TEM studies all showed the formation of dislocation loops and the high resistance of spinel against void formation. Possible reasons for the difference in dislocation-loop formation are differences in the neutron spectrum and neutron flux of the irradiation devices, or differences in the impurity contents, as has been discussed before. Kinoshita et al. [16] studied the influence of differences in the irradiation conditions. They compared the dislocation loop evolution in $MgAl_2O_4$ single crystals irradiated in the JOYO reactor and in the FFTF reactor and found that the evolution of the loops depends on the irradiation conditions. They suggested that this might be due to variations in the formation of transmutation elements in different reactors, which might influence the stacking fault energy and consequently the dislocation loop formation.

3.3. $Y_3Al_5O_{12}$

For the five $Y_3Al_5O_{12}$ pellets an average swelling of 0.5% has been obtained by measuring the dimensions. Hurley and Bunch [18] measured a 0.2% volume increase of polycrystalline $Y_3Al_5O_{12}$ and observed no volume change in $Y_3Al_5O_{12}$ single-crystals, both irradiated to a fluence of 2.8×10^{25} m^{-2} ($E > 0.1$ MeV) at 1015 K. In the present TEM investigation the formation of edge type dislocations, present as a set of dark parallel lines in the bright field images, is observed in some parts of the $Y_3Al_5O_{12}$ grains of the irradiated as well as the unirradiated material. Though they were observed more frequently in the irradiated material, it is not evident whether irradiation leads to growth of the dislocations. This might become clear from examination of samples irradiated to higher neutron fluences, which we will obtain from the EFTTRA-T2 experiment (total neutron fluence 2×10^{26}

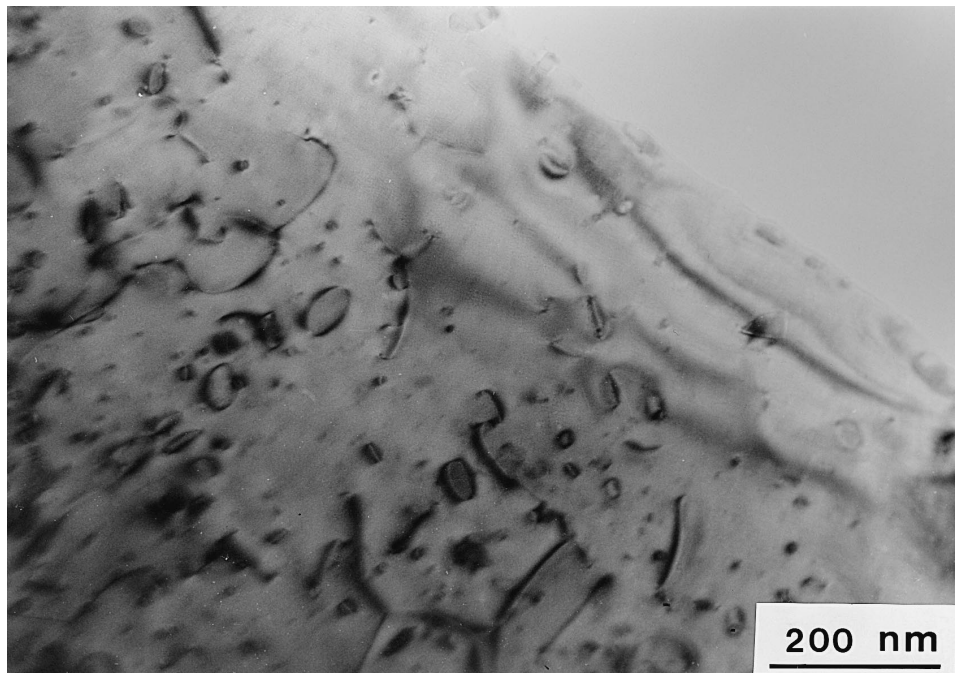

Fig. 4. TEM image of neutron irradiated CeO_2 (4.6×10^{25} m^{-2}).

m^{-2}). The results of TEM examinations on $Y_3Al_5O_{12}$ single-crystals irradiated at 925 K ($1–2 \times 10^{26}$ m^{-2}, $E >$ 0.1 MeV), 1015 K (0.3×10^{26} m^{-2}, $E > 0.1$ MeV) and 1100 K ($1–2 \times 10^{26}$ m^{-2}, $E > 0.1$ MeV) have been described by Clinard et al. [11]. They concluded that the TEM examinations showed no resolvable defect aggregates after the 1015 and 925 K irradiations, and only a sparse population of faulted {110} dislocation loops after the 1100 K exposure. Furthermore they concluded that a high concentration of unresolved mottled damage was evident, which would suggest that a significant fraction of the total displacement damage was retained in the lattice. Mitchell and Youngman [12] discussed the above mentioned TEM study on the $Y_3Al_5O_{12}$ samples irradiated at 1100 K and remarked that the Al_2O_3 phase present on the $Y_3Al_5O_{12}$ grain boundaries is full of dislocations and voids. They suggested that the swelling of the grain-boundary phase might strain the surrounding $Y_3Al_5O_{12}$ and wedge open cracks along the grain boundaries.

3.4. CeO_2

During the opening of the CeO_2 capsule it was observed that mechanical or chemical interaction had occurred between the stainless steel 316 L capsule and some of the CeO_2 pellets. By measuring the dimensions of the CeO_2 pellets an average volume change of -0.4% has been obtained. For these measurements only those pellets have been used in which the diameter was unaffected by the above mentioned interaction. Neutron irradiation of CeO_2 induces isolated dislocation loops, that can be observed on the TEM image (Fig. 4). The density of dislocation loops in CeO_2 is lower than that observed in Al_2O_3, and the average size is larger than that in Al_2O_3. No literature data on the swelling or the microstructure of neutron irradiated CeO_2 could be found. The only literature data available on the irradiation effects on CeO_2 is of Weber [19] and of Matzke et al. [20].

Weber studied the alpha-irradiation induced changes in the lattice parameter of CeO_2. It was observed that the alpha particles induce only a minor increase of the lattice parameter, which is comparable to the increase observed in UO_2 and PuO_2. Matzke et al. performed ion-implantation experiments at an energy of 72 MeV and observed that in CeO_2 the irradiation threshold above which important defects appear corresponds to 1.5% burnup (at 773 K).

4. Discussion

In the present study we have found that at the same irradiation temperature Al_2O_3 showed a significant and $Y_3Al_5O_{12}$ a slight swelling due to neutron irradiation. $MgAl_2O_4$ and CeO_2 in contrast showed a slight densification due to irradiation. The irradiation temperature is of course an important parameter, as has been discussed in the previous paragraphs, but has been the same for the materials studied here. Other parameters/effects that can influence the swelling behavior are, amongst others, lattice expansion, microcracking, the formation of dislocation

loops, the initial porosity structure and the grain size. In the present study no influence of lattice expansion and of microcracking could be observed. The influence of the initial porosity structure, the grain size and the formation of dislocation loops are discussed below in some more detail.

4.1. The initial porosity structure

Pores may act as vacancy sinks, in which case porosity enhances the swelling. In the case of UO_2 pellets it is observed that fission product spikes induce the disappearance of the fine initial porosity, which results in densification [22]. However, it is difficult to correlate the influence of fission product spikes with that of neutrons. The influence of neutron irradiation on the porosity structure of the presently studied samples is small. No changes in the porosity structure could be detected by comparison of the optical microscopy photographs that were made before and after irradiation.

4.2. The grain size

Clinard et al. [5] compared the irradiation behavior of single-crystalline and polycrystalline $MgAl_2O_4$. They observed that grain boundaries are effective sinks for interstitials, which allows void formation near the grain boundaries. This induces not only a difference between the swelling of single-crystalline and polycrystalline $MgAl_2O_4$, but it suggests also a difference between fine-grained and large-grained materials. In the present study swelling was observed for the Al_2O_3 and $Y_3Al_5O_{12}$ samples, that had a relatively small grain size, while for the $MgAl_2O_4$ and CeO_2 samples that had a relatively large grain size, densification was observed. However, the question whether a sample swells or densifies is not simply determined by its grain size. In the case of Al_2O_3 a direct relation between the grain size and swelling/densification does not exist since both polycrystalline materials and single-crystals show a comparable swelling during irradiation.

4.3. The formation of dislocation loops

The TEM analysis showed the formation of dislocation loops in Al_2O_3 and CeO_2, but the density of dislocation loops in Al_2O_3 is much higher than that in CeO_2 and the average size of the dislocation loops is smaller than that in CeO_2. No dislocation loops were found in $MgAl_2O_4$ and $Y_3Al_5O_{12}$. The difference in swelling rate and dislocation loop formation between $MgAl_2O_4$ and Al_2O_3 has been studied by several authors [10,16,23] and may be due to the difficult formation of low-energy stoichiometric dislocation loops in $MgAl_2O_4$ compared to Al_2O_3. Similar effects might be of importance for the behavior of $Y_3Al_5O_{12}$.

5. Conclusions

The neutron irradiation induced swelling and changes in the microstructure of Al_2O_3, $MgAl_2O_4$, $Y_3Al_5O_{12}$ and CeO_2 have been studied. The microstructure of $MgAl_2O_4$ and $Y_3Al_5O_{12}$ shows a good neutron irradiation stability and a high dimensional stability, which makes these compounds suitable inert-matrix candidates for actinide fuels. CeO_2 also shows a good dimensional stability during neutron irradiation, but due to the changes in the microstructure and the interaction with the stainless steel cladding it is less likely that CeO_2 can be used as an inert matrix. In the EFTTRA-T3 irradiation experiment, that is currently being performed in the HFR reactor, pellets of $MgAl_2O_4$, $Y_3Al_5O_{12}$ and CeO_2 containing UO_2 are being irradiated. This study will provide additional information on the applicability of $MgAl_2O_4$, $Y_3Al_5O_{12}$ and CeO_2 as inert matrices for actinide fuels. Al_2O_3 shows a considerable swelling and extensive dislocation-loop formation under neutron irradiation and consequently Al_2O_3 cannot be used as an inert matrix.

Acknowledgements

R. Belvroy, F. van den Berg, H. Buurveld, G. Dassel and W. Tams of the Hot-Cell Laboratory of ECN are acknowledged for performing the post-irradiation examinations.

References

[1] J.F. Babelot, R. Conrad, W.M.P. Franken, J. van Geel, H. Gruppelaar, G. Mühling, C. Prunier, M. Rome, M. Salvatores, Proc. of Global 95, 11–14 September, 1995, Versailles, France, p. 524.
[2] N. Cocuaud, E. Picard, R.J.M. Konings, A. Conti, Hj. Matzke, in: Proc. of GLOBAL'97, October 5–10, 1997, Yokohama, Japan, p. 1044.
[3] H.W. Chiang, R.N. Blumenthal, R.A. Fournelle, Solid State Ionics 66 (1993) 85.
[4] D.S. Tucker, T. Zocco, C.D. Kise, J.C. Kennedy, J. Nucl. Mater. 141–143 (1986) 401.
[5] F.W. Clinard Jr., G.F. Hurley, L.W. Hobbs, J. Nucl. Mater. 108&109 (1982) 655.
[6] W. Dienst, J. Nucl. Mater. 191–194 (1992) 555.
[7] G.W. Keilholtz, R.E. Moore, H.E. Robertson, Oak Ridge National Laboratory Report, ORNL-4678, 1971.
[8] F.W. Clinard Jr., J. Nucl. Mater. 85&86 (1979) 393.
[9] G.P. Pells, J. Am. Ceram. Soc. 77 (1994) 368.
[10] L.W. Hobbs, F.W. Clinard Jr., S.J. Zinkle, R.C. Ewing, J. Nucl. Mater. 216 (1994) 291.
[11] F.W. Clinard Jr., G.F. Hurley, R.A. Youngman, L.W. Hobbs, J. Nucl. Mater. 133&134 (1985) 701.
[12] T.E. Mitchell, R.A. Youngman, Proc. of the 7th Int. Conf. on High Voltage Electron Microscopy, Berkeley, 16–19 August, 1983, p. 163, Lawrence Berkeley Laboratory report, LBL-16031.

[13] G.F. Hurley, J.C. Kennedy, F.W. Clinard Jr., R.A. Youngman, W.R. McDonnel, J. Nucl. Mater. 103&104 (1981) 761.
[14] F.W. Clinard Jr., G.F. Hurley, L.W. Hobbs, D.L. Rohr, R.A. Youngman, J. Nucl. Mater. 122&123 (1984) 1386.
[15] K. Fukumoto, C. Kinoshita, F.A. Garner, J. Nucl. Sci. Technol. 32 (1995) 773.
[16] C. Kinoshita, K. Fukumoto, K. Fukuda, F.A. Garner, G.W. Hollenberg, J. Nucl. Mater. 219 (1995) 143.
[17] L.W. Hobbs, F.W. Clinard Jr., J. Phys. 41 (C6) (1980) 232.
[18] G.F. Hurley, J.M. Bunch, Am. Ceram. Soc. Bull. 59 (1980) 456.
[19] W.J. Weber, Radiat. Eff. 83 (1984) 145.
[20] Hj. Matzke, R.A. Verrall, P.G. Lucuta, Radiation damage in inert matrices by implantation of fission products of fission energy, J. Nucl. Mater., in press.
[21] L.W. Hobbs, J. Am. Ceram. Soc. 62 (1979) 267.
[22] W. Dörr, G. Maier, M. Peehs, J. Nucl. Mater. 106 (1982) 61.
[23] K. Tanimura, N. Itoh, F.W. Clinard, J. Nucl. Mater. 150 (1987) 182.
[24] F.W. Clinard, J.M. Bunch, W.A. Ranken, Los Alamos Report, LA-UR-75-1840, 1975.
[25] K. Nakai, K. Fukumoto, C. Kinoshita, J. Nucl. Mater. 191–194 (1992) 630.
[26] G.P. Pells, S.N. Buckley, P. Agnew, A.J.E. Foreman, M.J. Murphey, S.A.B. Staunton-Lambert, Harwell Laboratory Report, AERE-R-13222, 1988.